AD_____

Award Number: DAMD17-00-1-0091

TITLE: A Mouse Model for Prostate Cancer

PRINCIPAL INVESTIGATOR: Cory Abate-Shen, Ph.D.

CONTRACTING ORGANIZATION: University of Medicine and Dentistry
Robert Wood Johnson Medical School
Piscataway, New Jersey 08854-5635

REPORT DATE: July 2001

TYPE OF REPORT: Annual

PREPARED FOR: U.S. Army Medical Research and Materiel Command
Fort Detrick, Maryland 21702-5012

DISTRIBUTION STATEMENT: Approved for Public Release;
Distribution Unlimited

REPORT DOCUMENTATION PAGE

Form Approved
OMB No. 074-0188

1. AGENCY USE ONLY (Leave blank)	2. REPORT DATE	3. REPORT TYPE AND DATES COVERED
	July 2001	Annual (15 Jun 00 - 14 Jun 01)

4. TITLE AND SUBTITLE

A Mouse Model for Prostate Cancer

5. FUNDING NUMBERS

DAMD17-00-1-0091

6. AUTHOR(S)

Cory Abate-Shen, Ph.D.

7. PERFORMING ORGANIZATION NAME(S) AND ADDRESS(ES

University of Medicine and Dentistry
Robert Wood Johnson Medical School
Piscataway, New Jersey 08854-5635
E-Mail: abate@cabm.rutgers.edu

8. PERFORMING ORGANIZATION REPORT NUMBER

9. SPONSORING / MONITORING AGENCY NAME(S) AND ADDRESS(ES)

U.S. Army Medical Research and Materiel Command
Fort Detrick, Maryland 21702-5012

10. SPONSORING / MONITORING AGENCY REPORT NUMBER

11. SUPPLEMENTARY NOTES

Report contains color

12a. DISTRIBUTION / AVAILABILITY STATEMENT

Approved for Public Release; Distribution Unlimited

12b. DISTRIBUTION CODE

13. Abstract *(Maximum 200 Words)* *(abstract should contain no proprietary or confidential information)*

Mouse models of carcinogenesis have provided significant insights into the molecular mechanisms of tumor suppressor gene function. Our goal is to develop mouse models that recapitulate early stages of prostate carcinoma. Using such models we have demonstrated that the *Nkx3.1* homeobox gene represents a prostate-specific tumor suppressor that undergoes epigenetic inactivation through loss of protein expression. Loss-of-function of *Nkx3.1* in mice results in histopathological defects that resembles prostate cancer initiation in humans, and cooperates with loss-of-function of the *Pten* tumor suppressor gene in cancer progression. Furthermore, our findings suggest that the molecular mechanisms that mediate this cooperativity include the synergistic activation of Akt (protein kinase B), a key modulator of cell growth and survival. We propose that interactions between tissue-specific regulators such as *Nkx3.1* and broad-spectrum tumor suppressors such as *Pten* underlie the distinct phenotypes of different cancers.

14. SUBJECT TERMS	15. NUMBER OF PAGES
mouse models, tumor suppressor, PIN	27
	16. PRICE CODE

17. SECURITY CLASSIFICATION OF REPORT	18. SECURITY CLASSIFICATION OF THIS PAGE	19. SECURITY CLASSIFICATION OF ABSTRACT	20. LIMITATION OF ABSTRACT
Unclassified	Unclassified	Unclassified	Unlimited

Table of Contents

Cover	1
SF 298	2
Table of Contents	3
Introduction	4
Body	4-10
Key Research Accomplishments	11
Reportable Outcomes	11
Conclusions	11-12
References	13-15
Appendices	16

I. Introduction

Our **hypothesis** is that mouse models of prostate carcinogenesis can provide significant insights into the molecular mechanisms of tumor suppressor gene function, and our **primary goal** is to develop valid mouse models for early stages of the disease.

We have demonstrated that the *Nkx3.1* homeobox gene represents a prostate-specific tumor suppressor that undergoes epigenetic inactivation through loss of protein expression. Loss-of-function of *Nkx3.1* in mice results in histopathological defects that resemble prostate cancer initiation in humans, and cooperates with loss-of-function of the *Pten* tumor suppressor gene in cancer progression. Furthermore, our findings suggest that the molecular mechanisms that mediate this cooperativity include the synergistic activation of Akt (protein kinase B), a key modulator of cell growth and survival.

Our findings underscore the **significance** of interactions between tissue-specific regulators such as *Nkx3.1* and broad-spectrum tumor suppressors such as *Pten* underlie the distinct phenotypes of different cancers.

II. Body

A. Background and Significance

Molecular investigations of the functions of oncogenes and tumor suppressor genes have been greatly facilitated through the analysis of mouse models [1, 2] With respect to prostate carcinogenesis, mouse models can potentially overcome the inherent difficulties in studying the molecular genetics of this disease in humans [3-5]. In particular, human prostate cancer is characterized by the unusually long latency between the appearance of precursor lesions, termed prostatic intraepithelial neoplasia (PIN), which is relatively common in men in their twenties, and the manifestation of clinically detectable carcinomas that generally arise late in life. Thus, mouse models can provide insight into the molecular mechanisms involved in prostate cancer initiation and early steps of progression, which are otherwise nearly inaccessible in humans.

However, key anatomical and histological differences between the mouse and human prostate underscore the importance of validating the relevance of mouse models for human carcinogenesis [3]. For example, while the human prostate is a uni-lobular gland, the rodent prostate consists of distinct anterior, dorsolateral, and ventral lobes. Although the dorsolateral and anterior lobes are often considered to be analogous to the human peripheral zone (where prostate carcinomas arise), this comparison is primarily based on descriptive data. Despite these differences, recent analyses of mouse models have increasingly supported the view that the molecular pathways of prostate carcinogenesis are well-conserved between human and mouse (*e.g.,* [6-9], this work)

We have been utilizing mouse models to investigate the individual and collaborative roles of candidate tumor suppressor genes for prostate carcinogenesis. Our work has focused on the *Nkx3.1* homeobox gene because of its restricted expression in the developing and adult prostate and its essential role in prostate differentiation and function in mice [6, 10]. Furthermore, loss-of-function of *Nkx3.1* results in prostatic epithelial hyperplasia and dysplasia as a correlate of aging [6]. Moreover, *Nkx3.1* heterozygous mutants display a similar though less severe phenotype than the homozygotes, indicating haploinsufficiency [6].

The relevance of *NKX3.1* for human prostate cancer has been suggested by its localization to chromosomal region 8p21 [11, 12], which undergoes loss-of-heterozygosity (LOH) in approximately 80% of prostate cancers (*e.g.,* [13-16]). Notably, 8p21 LOH represents an early event in prostate carcinogenesis, since it occurs at high frequency in PIN lesions [14, 15], suggesting that genes within this region are involved in cancer initiation. However, the role of *NKX3.1* in human prostate carcinogenesis has been unclear, since it is not mutated in prostate cancer specimens [12]. Thus, while one allele of *NKX3.1* is

presumed to be lost in a high percentage of human prostate cancers, due to its localization to 8p21, the remaining allele does not undergo mutational inactivation.

In contrast to the prostate-specificity of *Nkx3.1*, *Pten* is broadly expressed during development and adulthood [17]. *Pten* encodes a lipid phosphatase that functions as an inhibitor of the PI3 kinase/Akt pathway ([18, 19] and reviewed in [20, 21]), and its essential function is evident from the early embryonic lethality of homozygous mutants [22-24]. In humans, *PTEN* maps to chromosomal region 10q23, which undergoes LOH at relatively advanced stages in many cancers [20, 21], suggesting that genes within this region are important for progression. Consistent with a tumor suppressor function, *PTEN* represents a frequent target of mutational inactivation in human cancers [20, 21], and *Pten* heterozygous mutant mice develop cancers of multiple tissues, including the prostate [7, 22, 24, 25].

Our current investigations of the roles of *Nkx3.1* and *Pten* in prostate carcinogenesis demonstrate that loss-of-function of a prostate-specific and of a broadly-expressed tumor suppressor gene can cooperate in prostate carcinogenesis. Moreover, our findings reveal an unexpected convergence of *Nkx3.1* and *Pten* functions in regulation of Akt activity.

B. Summary of Statement of work

Below we list our goals for this year (from the statement of work) and a brief description of the status. A detailed description of the results is presented in Section C (below):

Mouse breeding: generate compound mutants of *Nkx3.1* with *Pten* and *Mxi*: This goal has been successfully implemented.

Histopathological analysis of *Nkx3.1; Pten* and *Nkx3.1; Mxi* compound mutants: This goal has been successfully implemented. The histopathological phenotype of the *Nkx3.1; Pten* compound mutant mice are discussed in detail below. The *Nkx3.1; Mxi* compound mutants displayed no interesting phenotype, in fact the *Mxi* single mutants did not display any phenotype in the prostate (contrary to expectations based on the published report [26]. Therefore we have not further pursued analysis of *Mxi*.

Analysis of the role of *Pten* in the prostate: Our preliminary findings have not revealed a specific role for *Pten* in normal prostate development or function. However, these analysis should be facilitated by the generation of prostate-specific gene targeting of *Pten* using *Nkx3.1*-Cre mice that we have generated. These analyses will be a goal for the future years.

Cell culture analyses: As presented Section C, we have interesting findings regarding the individual and collaborative roles of *Nkx3.1* and *Pten* in synergistically activating Akt in prostate carcinoma cells.

Validation for human prostate cancer: As discussed in the Section C, our findings in the mouse model are strikingly reminiscent to the human disease.

C. Detailed discussion of major findings

Nkx3.1 mutant mice model human prostate cancer initiation: In our previous studies, we have found that homozygous and heterozygous *Nkx3.1* mutant mice develop prostatic epithelial hyperplasia and dysplasia prior to one year of age [6]. We have now observed a more severe phenotype in *Nkx3.1* mutants approaching two years of age (Fig. 1, Table 1). Notably, a majority of homozygotes (69%; n=11/16) and an intermediate number of heterozygotes (36%; n=4/11) develop histological features reminiscent of human PIN, including the appearance of cribriform or papillary architecture, atypical nuclei, and enlarged nucleoli (Fig. 1A-H; Table 1).These PIN regions in the *Nkx3.1* mutants display additional histopathological alterations that are characteristic of early-stage human prostate cancer (Fig. 1I-L) [3, 27]. In particular, the basal epithelium is absent in the PIN regions of the *Nkx3.1* mutants (Fig. 1I,J), reminiscent of the loss of the basal layer that is a hallmark of human prostate cancer. In addition, the stromal layer is significantly reduced in *Nkx3.1* mutants (Fig. 1K,L), indicative of an increased epithelial-stromal ratio. In contrast, *Nkx3.1* mutants display no increase in neuroendocrine cells (data not shown); such cells represent a small sub-population of epithelial cells that are sometimes amplified in more advanced stages of prostate carcinoma, but rarely in PIN [28]. These observations demonstrate that *Nkx3.1* mutant mice model key features of human prostate cancer initiation.

Tumor supressor activities of *Nkx3.1:* We have evaluated the potential tumor suppressor activities of *Nkx3.1* in prostate carcinoma cell lines using retroviral gene transfer (Fig. 2). To control for the consequences of overexpression versus specific effects on tumor suppression, we compared the activity of *Nkx3.1* to that of a mutated derivative, *Nkx3.1(L-S)*, which is inactive in DNA-binding and transcription assays (P. Sciavolino and C. A.-S., unpublished observations). In human (PC3) and rodent (AT6) prostate carcinoma cell lines [29, 30], which do not express the endogenous Nkx3.1 protein (Fig. 2A) [11], misexpression of *Nkx3.1*, but not *Nkx3.1(L-S)*, resulted in significant reductions in cellular proliferation, anchorage-independent growth, and tumor weight in *nude* mice (Fig. 2B-E). These tumor suppressor activities of *Nkx3.1* are consistent with the hyperplastic and dysplastic prostatic epithelium observed for *Nkx3.1* mutants [6].

Loss-of-function of *Nkx3.1* and *Pten* cooperate in prostate cancer progression: To examine whether loss-of-function of *Nkx3.1* and *Pten* collaborate in prostate carcinogenesis, we intercrossed compound heterozygotes (*Nkx3.1*$^{+/-}$; *Pten*$^{+/-}$) in a mixed C57Bl/6J-129/SvJ strain background to produce cohort groups comprised of all six viable genotypes (Fig. 3). Interestingly, our comparison of the prostatic phenotype of *Nkx3.1* and *Pten* single mutant mice (*Nkx3.1*$^{-/-}$; *Pten*$^{+/+}$ and *Nkx3.1*$^{+/+}$; *Pten*$^{+/-}$) at six months of age revealed notable histological differences. At this age, *Pten*$^{+/-}$ prostates displayed focal regions of severely dysplastic epithelium, unlike *Nkx3.1* mutants in which the prostatic epithelium was more broadly hyperplastic but less severely dysplastic (Fig. 1E-H, 3C,D,E,F,I,J). Moreover, *Nkx3.1* and *Pten* single mutants displayed somewhat different prostatic lobe specificities; the *Nkx3.1* phenotype was more severe in the anterior lobe, the *Pten* phenotype was more severe in the dorsolateral lobe, while neither mutant displayed any significant phenotype in the ventral lobe ([6] and data not shown).

Our analysis of the compound mutants revealed that loss-of-function of *Nkx3.1* and *Pten* displayed striking cooperativity in the anterior and dorsolateral prostatic lobes by 5 to 8 months of age (Figs. 3, 4; Table 2). In particular, *Nkx3.1*$^{+/-}$; *Pten*$^{+/-}$ and *Nkx3.1*$^{-/-}$; *Pten*$^{+/-}$ mice developed large focal lesions comprised of poorly differentiated cells with prominent and multiple nucleoli, increased nuclear:cytoplasmic ratio, and frequent mitotic figures (Fig. 3G,H,K,L). Notably, these lesions were larger and more prevalent in the *Nkx3.1*$^{-/-}$; *Pten*$^{+/-}$ mice as compared with the *Nkx3.1*$^{+/-}$; *Pten*$^{+/-}$ mice; similar, but significantly smaller, lesions were occasionally observed in aged-matched *Pten*$^{+/-}$ mice (Table 2).

These lesions were readily discernible as light-dense regions within the normally transparent prostatic ducts, usually filled the affected ducts, and were highly vascularized (Fig. 4A-D, I,J). Their histopathological features included a marked elevation and altered subcellular distribution of wide-spectrum cytokeratins, and an absence of basal epithelium (Fig. 4E-H). In addition, the lesions displayed a high proliferative index (~15%), as indicated by the prevalence of mitotic figures and the abundance of Ki67-labeled nuclei (Fig. 3L,4K,L). Based on their undifferentiated cytology, microvascularization, and high proliferative index, we have defined these lesions as prostatic carcinoma *in situ*.

Aside from the development of these prostatic carcinoma *in situ* lesions, the compound mutants (*Nkx3.1*$^{+/-}$; *Pten*$^{+/-}$ and *Nkx3.1*$^{-/-}$; *Pten*$^{+/-}$) displayed no additional phenotypes compared to the single mutants (*Nkx3.1*$^{-/-}$; *Pten*$^{+/+}$ and *Nkx3.1*$^{+/+}$; *Pten*$^{+/-}$). In particular, the compound mutants displayed a similar survival profile to the *Pten* single mutants (data not shown), which generally succumb to lymphomas and other non-prostate tumors by one year of age [22, 24, 25]. These findings are consistent with the prostate-specific phenotype of *Nkx3.1*, which does not have an impact on survival rate. Furthermore, these observations emphasize the prostate-specificity of the cooperativity between loss-of-function of *Nkx3.1* and *Pten*.

Absence of Nkx3.1 protein expression in mouse and human prostate cancer: Since carcinoma *in situ* lesions frequently occurred in *Nkx3.1*$^{+/-}$; *Pten*$^{+/-}$ compound mutants, which are heterozygous for *Nkx3.1*, we examined the status of *Nkx3.1* expression in these lesions (Fig. 5). Strikingly, our immunohistochemical analysis revealed that Nkx3.1 protein expression was invariably absent from the carcinoma *in situ* lesions of the compound heterozygotes (100% n=25) (Fig. 5D). This absence of staining contrasted with the robust nuclear staining in regions of relatively normal ("unaffected") histology adjacent to the lesions. In some cases, particularly at the margins of relatively large lesions, we observed mislocalization of Nkx3.1 protein to the cytoplasm (Fig. 5F), which may provide an alternative means for inactivating *Nkx3.1* function.

More generally, we have found that the absence of Nkx3.1 protein expression is a common feature of PIN and carcinoma *in situ* lesions in our single and compound mutant mice. For example, Nkx3.1 protein expression was absent in the relatively small carcinoma *in situ* lesions found in *Pten*$^{+/-}$ single

mutants, which are genotypically wild-type for *Nkx3.1* (Fig. 5C). We have also found that loss of Nkx3.1 protein expression was a common occurrence in PIN regions of *Nkx3.1* heterozygotes (which are wild-type for *Pten)* (Fig. 5B). Finally, we have observed absence of Nkx3.1 immunostaining in small clusters of cells with relatively normal histology in both *Nkx3.1* heterozygotes and in *Nkx3.1; Pten* compound heterozygotes (Fig. 5E), suggesting that Nkx3.1 protein loss precedes formation of PIN or carcinoma *in situ*, respectively.

In a parallel analyses of human prostate cancer, we observed that NKX3.1 protein expression was significantly reduced (56%; n=15/27) or absent (26%; n=7/27) in a majority of cancer specimens, with an occasional shift from nuclear to cytoplasmic subcellular localization (11%; n=3/27) (Fig. 5G-I). These findings are in accordance with a recent report demonstrating the frequent reduction or absence of NKX3.1 protein expression in a large-scale analysis of tissue arrays from human prostate cancer specimens. Thus, loss and/or mislocalization of NKX3.1 protein expression is characteristic of prostate carcinogenesis in the *Nkx3.1; Pten* mouse model as well as in humans.

***Pten*, but not *Nkx3.1*, undergoes allelic loss in carcinoma *in situ* lesions from compound mutants:** To examine the status of the wild-type *Nkx3.1* and *Pten* alleles in the carcinoma *in situ* lesions of the compound heterozygotes, we performed laser-capture microdissection on Nkx3.1-immunostained sections to recover genomic DNA from the carcinoma *in situ* lesions (Nkx3.1 non-expressing) and adjacent unaffected regions (Nkx3.1-expressing) (Fig. 5M). In all cases analyzed, the wild-type *Nkx3.1* allele was retained (n=20 Nkx3.1 non-expressing lesions and 8 Nkx3.1-expressing controls); moreover, no mutations were detected in the *Nkx3.1* coding region (Fig. 5N and data not shown). Despite the absence of Nkx3.1 protein expresion, *Nkx3.1* mRNA expression was readily detected by RT-PCR as well as *in situ* hybridization (data not shown).

In contrast, *Pten* sustained allelic loss in 9 out of 10 carcinoma *in situ* lesions from *Nkx3.1; Pten* compound heterozygotes (Fig. 5O and data not shown); this was accompanied by a loss of Pten protein expression, which was apparent both by immunohistochemistry and by Western blotting (Figs. 5L, 6A). Interestingly, *Pten* did not undergo allelic loss in adjacent unaffected regions (Fig. 5O), and Pten protein expression was only modestly reduced in the relatively small lesions of the $Pten^{+/-}$ mice (Figs. 5K). Our findings demonstrate that *Pten* undergoes LOH within carcinoma *in situ* lesions of *Nkx3.1; Pten* compound mutant mice, and help to reconcile discrepancies in the literature regarding the allelic status of *Pten* in mutant mouse models [7, 25].

Synergistic activation of Akt by loss-of-function of Nkx3.1 and *Pten*: Finally, we examined the biochemical mechanism for the observed cooperativity between *Nkx3.1* and *Pten* by investigating whether these genes affect a common signaling pathway. Since *Pten* is known to inhibit activation of the Akt kinase [31-33] and reviewed in [21, 34, 35], we examined the expression levels and distribution of activated Akt in single and compound mutant prostates using an antibody specific for the activated (phosphorylated) form (Fig. 6).

By Western blot analysis, we observed a marked increase in activated Akt in the $Nkx3.1^{-/-}$; $Pten^{+/-}$ compound mutant prostates relative to the wild-type or single mutants, although the level of total Akt protein was equivalent in animals of all genotypes (n=9, Fig. 6A). Moreover, Akt activation was restricted to the prostate and was not observed in tissues that do not express *Nkx3.1*, such as the bladder (Fig. 6A). Activation of Akt in the compound mutants was detected as early as 2 months of age, preceding the formation of overt carcinoma *in situ* lesions (data not shown). These observations are consistent with the idea that activation of Akt in the compound mutant prostates was due to synergism between loss-of-function of *Nkx3.1* and *Pten*.

Immunohistochemical analysis revealed robust phospho-Akt staining in the carcinoma *in situ* lesions of *Nkx3.1; Pten* compound mutants and *Pten* single mutants (n=30, Fig. 6E). In addition, we detected phospho-Akt staining in small clusters of cells with relatively normal histology in both the $Pten^{+/-}$ single and *Nkx3.1; Pten* compound mutants (Fig. 6D); interestingly, a majority of these phospho-Akt positive foci arising in the $Nkx3.1^{+/-}$; $Pten^{+/-}$ compound heterozygotes lacked Nkx3.1 immunostaining (data not shown).

We also observed phospho-Akt staining in the prostatic epithelium of *Nkx3.1* single mutants, suggesting that loss-of-function of *Nkx3.1* can affect Akt activation in the context of wild-type *Pten* function (n=13, Fig. 6F-H). Activated Akt immunostaining was relatively restricted in its distribution, and was typically detected in isolated clusters of epithelial cells in *Nkx3.1* homozygous and heterozygous mutants.

These phospho-Akt-expressing clusters were generally found near ductal tips and were correlated with the presence of PIN; notably, they were immunopositive for Pten (data not shown). Although prevalent in the prostate of the *Nkx3.1* mutants, phospho-Akt staining was not detected in other epithelial tissues from these mutants, such as bladder and intestine (data not shown).

While we occasionally detected phospho-Akt staining associated with the cell surface in the *Nkx3.1* mutants (Fig. 6F), we more often observed that phospho-Akt distribution was primarily nuclear in these mutants (Fig. 6H). Furthermore, overexpression of *Nkx3.1* in LNCaP prostate carcinoma cells, which lack functional *PTEN* [36], resulted in enrichment of total and activated Akt protein in the cytoplasmic compartment, as measured by Western blotting and kinase activity assays (Fig. 6B). This effect of Nkx3.1 on Akt subcellular localization is noteworthy since Akt is activated at the cell membrane and it is subsequently translocated to the nucleus, where it has been proposed to phosphorylate regulatory targets [37-39]. In summary, our findings indicate that loss-of-function of *Nkx3.1* and *Pten* converge on Akt activation, and implicate *Nkx3.1* as a regulator of Akt subcellular distribution.

D. Experimental Methods

Cell Culture Assays: Sequences corresponding to the coding region of *Nkx3.1* [10] were subcloned into *pLZRSΔ-IRES-GFP,* a derivative of *LZRSpBMN-Z* [40] in which the *lacZ* gene was replaced with an *IRES-GFP* cassette. The *Nkx3.1(L-S)* mutant contains a substitution of leucine 140 to serine (position 16 of the homeodomain) that was introduced by PCR mutagenesis. Replication-defective mammalian retroviruses were made in Phoenix amphitropic retroviral packaging cells (ATCC). Target cells were seeded at a density of 1 x 10^4/cm^2 for PC3 cells and 5 X 10^3/cm^2 for AT6 (AT6.3, [30]) cells, and infected with viral supernatants (containing 8 μg/ml polybrene) on three consecutive days. Following isolation of the GFP-expressing cells by flow cytometry, greater than 95% of the cells expressed GFP as well as high levels of Nkx3.1 protein (Fig. 2A and data not shown). Expression of Nkx3.1 or Nkx3.1(L-S) was verified by Western blot analysis directly following flow cytometry, and also at the termination of each assay.

Following retroviral gene transfer and cell sorting, PC3 and AT6 cells [29, 30] were seeded in triplicate at a density of 5 X 10^3/cm^2 or 1 X 10^3/ cm^2, respectively, in low-serum media (0.5% or 0.25%, respectively); media was replenished every second day. At the indicated days, cell number was determined by optical density following staining with Napthol blue black (Sigma). Anchorage-independent growth was monitored by seeding AT6 cells in triplicate at a density of 1 X 10^3/ cm^2, in media containing 0.35% agarose layered over 0.5% agar. Following growth for 14 days, the number of GFP-expressing colonies was determined by counting under a fluorescence microscope. Tumor growth in *nude* mice (Taconic) was monitored by subcutaneous injection of AT6 (1 X 10^4) or PC3 (1 X 10^6 in 50% matrigel) cells. Tumor size was monitored once per week for four (AT6) or six (PC3) weeks by caliper measurement, followed by determination of tumors weights at necropsy. Expression of Nkx3.1 protein in the tumors was verified by immunohistochemistry. Statistical analyses were performed using a two-sample *t* test for independent samples with unequal variances (Satterthwaite's method).

Histological analyses: We analyzed paraffin-embedded human prostate tumor specimens retrieved from the surgical pathology files at the University of California Davis Medical Center (generously supplied by Dr. Regina Gandour-Edwards). The histological diagnosis and Gleason grade were independently verified by one of us (R.D.C.) and Dr. Gandour-Edwards. The anti-NKX3.1 antisera was generated using as an antigen NKX3.1 full-length protein that was purified from *E. coli* by hexa-histidine affinity chromatography. The data shown were performed using anti-NKX3.1 polyclonal antisera; similar results were obtained with an anti-NKX3.1 monoclonal antibody (data not shown). Immunodetection was performed using Vector Elite ABC kit Rabbit IgG with Vector *NovaRED* substrate kit (Vector Laboratories).

For histological analyses of mouse tissues, dissected tissues were fixed in 10% formalin, embedded in paraffin, and processed for hematoxylin-and-eosin staining. The primary histological analysis was performed on a non-blinded basis (by R.D.C.); one of us (M.M.S.) independently reviewed the histological data on a blinded basis, reaching similar conclusions.

Immunohistochemical analysis was performed on 4% paraformaldehyde-fixed cryosections (for Akt and phospho-Akt antibodies) or formalin-fixed paraffin sections following antigen retrieval (for all other antibodies). Antibodies were: monoclonal antibody against smooth muscle actin (Sigma); monoclonal antibody against cytokeratin 14 (Biogenex); monoclonal antibody against CD105/endoglin (DAKO);

polyclonal antisera against poly-cytokeratins, for wide-spectrum screening (CK-P, DAKO); polyclonal antisera against Ki67 antigen (Novocastra Laboratories); polyclonal antisera against PTEN/MMAC1 (Ab-2, NeoMarkers); polyclonal antisera against Akt and phospho-Akt (Ser 473) (Cell Signaling Technology). The anti-mouse Nkx3.1 antisera were generated using as an antigen the full-length Nkx3.1 protein purified from *E. coli* by hexa-histidine affinity chromatography. Immunodetection of monoclonal antibodies was performed using Vector M.O.M. kit and for polyclonal antisera with a Vector Elite ABC kit for Rabbit IgG; for substrate detection we used a Vector *NovaRED* kit (all from Vector Laboratories). Ki67-labelled nuclei were quantitated by counting approximately 20,000 hematoxylin-stained nuclei from high-power microscopic fields.

Laser-capture microdissection was performed on Nkx3.1-immunostained sections using a PixCell apparatus (Arcturus Eng. Inc). We pooled 1000 laser pulses from independent lesions and extracted genomic DNA at 37°C overnight in buffer containing 50mM Tris-HCl (pH 8.5), 0.5% Tween-20, 1mM EDTA (pH 8.0), and 0.5 mg/ml Proteinase K. DNA was analyzed by PCR amplification followed by Southern blotting. Primer sequences were as follows: *Nkx3.1* wild type allele, 5'-GCCACAGTGGCTGATGTCAAGGAGTCGG (primer A) and 5'–GCCAACCTGCCTCAATCACTAAGG; *Nkx3.1* targeted allele, primer A and 5'-TTCCACATACACTTCATTCTCAGT; *Pten* wild type allele (exon 5), 5'–AAAAGTCAGTCTTTTCCATAGTTGA (primer B) and 5'–AATATAACAGTTCTCAAAGCATCA; *Pten* targeted allele, primer B and 5'-TAGCGCCAAGTGCCCAGCGGGGC. The probes for Southern blotting were: *Nkx3.1* 3'UTR (WT), *Pten* exon 5 (WT) and the neo cassette (KO for *Nkx3.1* and *Pten*).

Analysis of Akt activity: Total protein extracts were prepared by sonication followed by centrifugation of dissected anterior prostates in 600 µl of buffer A, containing 20 mM Hepes, pH 7.4, 450 mM NaCl, 0.2 mM EDTA, 0.5 mM DTT, 25% glycerol, and protease inhibitor and phosphatase inhibitor cocktails (Sigma p2714, p2850). Following retroviral gene transfer, LNCaP cells were lysed in buffer A for whole cell extracts. For cytoplasmic extracts, cells were lysed in buffer containing 20mM Hepes, pH 7.4, 5 mM NaCl, 10 mM MgCl, 1 mM EDTA, 1 mM DTT, and protease inhibitor and phosphatase inhibitor cocktails (Sigma p2714, p2850). Following centrifugation of the cytoplasmic lysates, nuclear proteins were extracted from the pellet using buffer A. Akt kinase assays were performed using 100 µg of whole cell, cytoplasmic or nuclear extracts using a non-radioactive IP-kinase assay kit from Cell Signaling Technology.

E. Tables

Table 1: Summary of epithelial defects in the anterior prostate of *Nkx3.1* mutant mice[a]

Genotype	Total #	Normal	Hyperplasia	PIN
+/+				
1-6 month	N=11	11	0	0
6-12 month	N=6	4	1	1
12-24 month	N=11	9	2	0
	N=28	**24**	**3**	**1**
+/-				
1-6 month	N=12	9	3	0
6-12 month	N=7	2	2	3
12-24 month	N=11	3	4	4
	N=30	**14**	**9**	**7**
-/-				
1-6 months	N=13	2	5	6
6-12 month	N=9	3	1	5
12-24 month	N=16	0	5	11
	N=38	**5**	**11**	**22**

a) Data for the mice at 1-12 months includes data previously reported in [6].

Table 2: Summary of the prostatic epithelial defects in *Nkx3.1;Pten* compound mutant mice at 5-8 months of age

Genotype	Total #	Normal	Hyperplasia	PIN	Carcinoma *in situ*
***Nkx3.1*$^{+/+}$;Pten$^{+/+}$**	N=6	5	1	0	0
***Nkx3.1*$^{+/-}$;Pten$^{+/+}$**	N=11	6	4	1	0
***Nkx3.1*$^{-/-}$;Pten$^{+/+}$**	N=10	2	4	4	0
***Nkx3.1*$^{+/+}$;Pten$^{+/-}$**	N=10	3	2	5	2
***Nkx3.1*$^{+/-}$;Pten$^{+/-}$**	N=13	2	3	8	8
***Nkx3.1*$^{-/-}$;Pten$^{+/-}$**	N=11	0	2	9	11

III. Key Research Accomplishments

- *Nkx3.1* mutant mice develop histopathological features of human prostate cancer initiation as a correlate of aging (Fig. 1, Table 1)
- *NKX3.1* displays tumor suppressor activities in cell culture and in *nude* mice (Fig. 2)
- Loss-of-function of *Nkx3.1* and *Pten* cooperate in prostate carcinogenesis that us manifested by the appearance of carcinoma *in situ* lesions in compound mutant mice (Figs. 3 and 4)
- *NKX3.1* undergoes epigenetic inactivation in prostate cancer in mouse models and human cancer (Fig. 5)
- *Pten*, but not *Nkx3.1*, undergoes allelic loss in carcinoma *in situ* lesions of compound mutant mice (Fig. 5)
- Mechanism of cooperativity by *Nkx3.1* and *Pten* is mediated in part by synergistic activation of Akt (Fig. 6)
- *Nkx3.1* affects the subcellular distribution of Akt in animal models and *in vitro* (Fig. 6)

IV. Reportably Outcomes

- Patents pending:
  - 1. Roles for *Nkx3.1* in prostate development and cancer
  - Monoclonal Antibodies for *Nkx3.1* and method for detecting same
- Reagents developed:
  - Monoclonal and polyclonal antisera against human *NKX3.1*
  - Polyclonal antisera against mouse *Nkx3.1*
- Manuscripts:
  - "Cooperativity of tissue-specific and broad-spectrum tumor suppressor genes in a mouse model of prostate carcinogenesis" Kim, M., Cardiff, R. Desai, N., Banach, W., Bhatia-Gaur, R., Shen, M., and Abate-Shen, C. (submitted)

V. Conclusions

Until recently, the validity of the mouse as a model for human prostate cancer has been controversial, due to the anatomical and histological differences between mouse and human prostate and the absence of spontaneous prostate cancer in the mouse (reviewed in [3-5]. Our findings demonstrate the utility of mutant mouse models for recapitulating early stages of human prostate carcinogenesis and for providing novel mechanistic insights into this process.

Several lines of evidence implicate *NKX3.1* as a tumor suppressor gene whose loss-of-function represents a critical step in prostate cancer initiation. First, *NKX3.1* displays tumor suppressor activities in cell culture and in *nude* mice. Secondly, *Nkx3.1* mutant mice develop PIN, paralleling the predicted consequences of chromosome 8p21 LOH in human prostate carcinogenesis. Finally, the *NKX3.1* locus is contained within a minimal deletion interval (~1500 kb) of human chromosome 8p21 that has been defined by allelotyping studies of prostate carcinomas (M. Emmert-Buck, personal communication).

Furthermore, the epigenetic inactivation of *NKX3.1* function through loss of protein expression is a hallmark of prostate cancer in humans and in mutant mouse models ([41]; unpublished observations).

Notably, this loss of protein expression occurs without accompanying loss of mRNA expression or mutational inactivation of the *NKX3.1* locus [12, 42, 43]. One possible mechanism for loss of NKX3.1 protein expression is altered translational or post-translational control, potentially involving the unusually long (~4 kb) *NKX3.1* 3' UTR [10]; an alternative possibility is de-regulated intracellular transport and/or degradation, which would account for cytoplasmic localization of NKX3.1 protein. Regardless of the mechanism, the observed absence of Nkx3.1 protein expression provides an explanation for the haploinsufficient phenotype of *Nkx3.1* heterozygous mice, and reconciles a crucial role for *NKX3.1* in human prostate cancer with the failure to detect inactivating mutations.

In contrast to the prostate-specificity of *NKX3.1, PTEN* is a broad-spectrum tumor suppressor gene whose loss-of-function through mutational inactivation has been implicated in many different cancers. In our studies of compound mutant mice, we have observed that loss-of-function of *Nkx3.1* and *Pten* display cooperativity in carcinogenesis of the prostate, but not other tissues. This contrasts with the consequences of loss-of-function of *Pten* and the cyclin-dependent kinase inhibitor, $p27^{KIP1}$, which display cooperativity in carcinogenesis of the prostate as well as many other tissues [7]. Although the cumulative data from human studies indicate that loss-of-function of *NKX3.1* corresponds to an initiation event in prostate carcinogenesis, whereas loss of *PTEN* corresponds to a progression event, a primary limitation of our mouse model is the inability to provide insight into the sequential order of events. Thus, while our current studies have elucidated genetic components of a prostate cancer progression pathway, future studies using inducible targeting strategies or similar approaches will be necessary to explore the physiological sequence of events.

The convergence of the *Nkx3.1* and *Pten* mutant phenotypes on Akt activation in the prostate implies that de-regulation of Akt activity is a critical event in prostate carcinogenesis, consistent with the recent observation of elevated phospho-Akt levels in human PIN [44] Notably, however, the non-uniform activation of Akt in the prostatic epithelium of *Nkx3.1* mutants indicates that this activation represents an indirect consequence of *Nkx3.1* loss-of-function. In particular, our findings suggest that *Nkx3.1* may directly affect the nuclear-cytoplasmic distribution of Akt protein, which may have indirect consequences for its ability to become activated. This effect of *Nkx3.1* on Akt subcellular localization is unlikely to be mediated by the PI3 kinase pathway, since it is unaffected by PI3 kinase inhibitors (unpublished data). Thus, we speculate that *Nkx3.1* plays a role in regulating Akt activity that is independent of the PI3 kinase pathway and PTEN function.

In conclusion, we have shown that collaboration between a tissue-specific modulator of prostatic epithelial differentiation and a broad-spectrum tumor suppressor gene can contribute to cancer progression. These observations raise the possibility that the apparent tissue-selectivity of broad-spectrum tumor suppressors [1, 2] may be generated through their synergy with tissue-specific genes to affect common signaling pathways, such as what we have observed for *Pten* and *Nkx3.1* upon Akt activation in the prostate. Thus, we propose that these collaborative interactions contribute to the distinguishing features of prostate carcinoma, and that similar interactions may generally explain the tissue-specific phenotypes of cancers.

VI. References

1. Jacks, T., *Tumor suppressor gene mutations in mice.* Annu Rev Genet, 1996. **30**: p. 603-36.

2. Macleod, K.F. and T. Jacks, *Insights into cancer from transgenic mouse models.* J Pathol, 1999. **187**(1): p. 43-60.

3. Abate-Shen, C. and M.M. Shen, *Molecular genetics of prostate cancer.* Genes Dev, 2000. **14**(19): p. 2410-34.

4. Matusik, R., et al., *Transgenic mouse models of prostate cancer,* in *Transgenics in Endocrinology,* M. Matzuk, C. Brown, and T. Kumar, Editors. 2001 (In press), The Humana Press, Inc.: Totowa, NJ.

5. Green, J.E., et al., *Workgroup 3: transgenic and reconstitution models of prostate cancer.* Prostate, 1998. **36**(1): p. 59-63.

6. Bhatia-Gaur, R., et al., *Roles for Nkx3.1 in prostate development and cancer.* Genes Dev, 1999. **13**(8): p. 966-77.

7. Di Cristofano, A., et al., *Pten and p27KIP1 cooperate in prostate cancer tumor suppression in the mouse.* Nat Genet, 2001. **27**(2): p. 222-4.

8. Huss, W.J., et al., *Angiogenesis and prostate cancer: identification of a molecular progression switch.* Cancer Res, 2001. **61**(6): p. 2736-43.

9. Masumori, N., et al., *A probasin-large T antigen transgenic mouse line develops prostate adenocarcinoma and neuroendocrine carcinoma with metastatic potential.* Cancer Res, 2001. **61**(5): p. 2239-49.

10. Sciavolino, P.J., et al., *Tissue-specific expression of murine Nkx3.1 in the male urogenital system.* Dev Dyn, 1997. **209**(1): p. 127-38.

11. He, W.W., et al., *A novel human prostate-specific, androgen-regulated homeobox gene (NKX3.1) that maps to 8p21, a region frequently deleted in prostate cancer.* Genomics, 1997. **43**(1): p. 69-77.

12. Voeller, H.J., et al., *Coding region of NKX3.1, a prostate-specific homeobox gene on 8p21, is not mutated in human prostate cancers.* Cancer Res, 1997. **57**(20): p. 4455-9.

13. Bergerheim, U.S., et al., *Deletion mapping of chromosomes 8, 10, and 16 in human prostatic carcinoma.* Genes Chromosomes Cancer, 1991. **3**(3): p. 215-20.

14. Emmert-Buck, M.R., et al., *Allelic loss on chromosome 8p12-21 in microdissected prostatic intraepithelial neoplasia.* Cancer Res, 1995. **55**(14): p. 2959-62.

15. Haggman, M.J., et al., *Allelic loss of 8p sequences in prostatic intraepithelial neoplasia and carcinoma.* Urology, 1997. **50**(4): p. 643-7.

16. Vocke, C.D., et al., *Analysis of 99 microdissected prostate carcinomas reveals a high frequency of allelic loss on chromosome 8p12-21.* Cancer Res, 1996. **56**(10): p. 2411-6.

17. Luukko, K., et al., *Expression of LKB1 and PTEN tumor suppressor genes during mouse embryonic development.* Mech Dev, 1999. **83**(1-2): p. 187-90.

18. Maehama, T. and J.E. Dixon, *The tumor suppressor, PTEN/MMAC1, dephosphorylates the lipid second messenger, phosphatidylinositol 3,4,5-trisphosphate.* J Biol Chem, 1998. **273**(22): p. 13375-8.

19. Myers, M.P., et al., *The lipid phosphatase activity of PTEN is critical for its tumor supressor function.* Proc Natl Acad Sci U S A, 1998. **95**(23): p. 13513-8.

20. Cantley, L.C. and B.G. Neel, *New insights into tumor suppression: PTEN suppresses tumor formation by restraining the phosphoinositide 3-kinase/AKT pathway.* Proc Natl Acad Sci U S A, 1999. **96**(8): p. 4240-5.

21. Di Cristofano, A. and P.P. Pandolfi, *The multiple roles of PTEN in tumor suppression.* Cell, 2000. **100**(4): p. 387-90.

22. Di Cristofano, A., et al., *Pten is essential for embryonic development and tumour suppression.* Nat Genet, 1998. **19**(4): p. 348-55.

23. Suzuki, A., et al., *High cancer susceptibility and embryonic lethality associated with mutation of the PTEN tumor suppressor gene in mice.* Curr Biol, 1998. **8**(21): p. 1169-78.

24. Podsypanina, K., et al., *Mutation of Pten/Mmac1 in mice causes neoplasia in multiple organ systems.* Proc Natl Acad Sci U S A, 1999. **96**(4): p. 1563-8.

25. Stambolic, V., et al., *High incidence of breast and endometrial neoplasia resembling human Cowden syndrome in pten+/- mice.* Cancer Res, 2000. **60**(13): p. 3605-11.

26. Schreiber-Agus, N., et al., *Role of Mxi1 in ageing organ systems and the regulation of normal and neoplastic growth.* Nature, 1998. **393**(6684): p. 483-7.

27. Bostwick, D.G., *Prospective origins of prostate carcinoma. Prostatic intraepithelial neoplasia and atypical adenomatous hyperplasia.* Cancer, 1996. **78**(2): p. 330-6.

28. Abrahamsson, P.A., *Neuroendocrine differentiation in prostatic carcinoma.* Prostate, 1999. **39**(2): p. 135-48.

29. Kaighn, M.E., et al., *Establishment and characterization of a human prostatic carcinoma cell line (PC-3).* Invest. Urol., 1979. **17**: p. 16-23.

30. Isaacs, J.T., et al., *Establishment and characterization of seven Dunning rat prostatic cancer cell lines and their use in developing methods for predicting metastatic abilities of prostatic cancers.* Prostate, 1986. **9**(3): p. 261-81.

31. Stambolic, V., et al., *Negative regulation of PKB/Akt-dependent cell survival by the tumor suppressor PTEN.* Cell, 1998. **95**(1): p. 29-39.

32. Wu, X., et al., *The PTEN/MMAC1 tumor suppressor phosphatase functions as a negative regulator of the phosphoinositide 3-kinase/Akt pathway.* Proc Natl Acad Sci U S A, 1998. **95**(26): p. 15587-91.

33. Sun, H., et al., *PTEN modulates cell cycle progression and cell survival by regulating phosphatidylinositol 3,4,5,-trisphosphate and Akt/protein kinase B signaling pathway.* Proc Natl Acad Sci U S A, 1999. **96**(11): p. 6199-204.

34. Coffer, P.J., J. Jin, and J.R. Woodgett, *Protein kinase B (c-Akt): a multifunctional mediator of phosphatidylinositol 3-kinase activation.* Biochem J, 1998. **335**(Pt 1): p. 1-13.

35. Datta, S.R., A. Brunet, and M.E. Greenberg, *Cellular survival: a play in three Akts.* Genes Dev, 1999. **13**(22): p. 2905-27.

36. Li, J., et al., *PTEN, a putative protein tyrosine phosphatase gene mutated in human brain, breast, and prostate cancer [see comments].* Science, 1997. **275**(5308): p. 1943-7.

37. Meier, R., et al., *Mitogenic activation, phosphorylation, and nuclear translocation of protein kinase Bbeta.* J Biol Chem, 1997. **272**(48): p. 30491-7.

38. Andjelkovic, M., et al., *Role of translocation in the activation and function of protein kinase B.* J Biol Chem, 1997. **272**(50): p. 31515-24.

39. Brunet, A., et al., *Akt promotes cell survival by phosphorylating and inhibiting a Forkhead transcription factor.* Cell, 1999. **96**(6): p. 857-68.

40. Kinsella, T.M. and G.P. Nolan, *Episomal vectors rapidly and stably produce high-titer recombinant retrovirus.* Hum Gene Ther, 1996. **7**(12): p. 1405-13.

41. Bowen, C., et al., *Loss of NKX3.1 expression in human prostate cancers correlates with tumor progression [In Process Citation].* Cancer Res, 2000. **60**(21): p. 6111-5.

42. Ornstein, D.K., et al., *Expression studies and mutational analysis of the androgen regulated homeobox gene NKX3.1 in benign and malignant prostate epithelium.* J Urol, 2001. **165**(4): p. 1329-34.

43. Xu, L.L., et al., *Expression profile of an androgen regulated prostate specific homeobox gene NKX3.1 in primary prostate cancer.* J Urol, 2000. **163**(3): p. 972-9.

44. Paweletz, C.P., et al., *Reverse phase protein microarrays which capture disease progression show activation of pro-survival pathways at the cancer invasion front.* Oncogene, 2001. **20**(16): p. 1981-9.

APPENDIX

- Biosketch, Cory Abate-Shen (PI)
- Figures legends
- Figures 1-6

BIOGRAPHICAL SKETCH

NAME	POSITION TITLE
Cory Abate-Shen	Professor

EDUCATION *(Begin with baccalaureate or other initial professional education, such as nursing, and include postdoctoral training.)*

INSTITUTION AND LOCATION	DEGREE	YEAR CONFERRED	FIELD OF STUDY
Fordham University	B.A.	1983	Psychology
Cornell University Medical College	Ph.D.	1988	Neurobiology
Roche Institute of Molecular Biology	post doc	1988-1991	Gene Regulation

RESEARCH AND/OR PROFESSIONAL EXPERIENCE: Concluding with present position, list in chronological order previous employment, experience, and honors. Include present membership on any Federal Government public advisory committee. Specify the total number of publications and list, in chronological order, the titles, all authors, and complete references to all publications during the past three years and to representative earlier publications pertinent to this application. DO NOT EXCEED TWO PAGES.

Professional Experience:

1983 - 1988 Graduate Research Assistant, Laboratory of Molecular Neurobiology, Cornell University
1988 - 1990 Postdoctoral Fellow, Molecular Oncology & Virology, Roche Inst. of Molecular Biology
1991 - 1991 Research Fellow, Molecular Oncology & Virology, Roche Inst. of Molecular Biology
1991 - 1997 Assistant Professor, Neuroscience and Cell Biology, UMDNJ
1997 - 2001 Associate Professor, Neuroscience and Cell Biology, UMDNJ
1991 - present Resident Member, Center for Advanced Biotechnology and Medicine
2001 - present Professor, Neuroscience and Cell Biology, UMDNJ
1995 - present Member, The Cancer Institute of New Jersey
1999 - present Scientific Director, The Dean and Betty Gallo Prostate Cancer Institute

Honors and Awards:

1983 Summa Cum Laude, Fordham University
1987 Vincent du Vigneaud Award for Excellence in Graduate Research, Cornell University Medical College
1992-1995 Sinsheimer Scholar Award
1993-1998 NSF Young Investigator Award
1993 Women in Cell Biology Junior Award, American Society for Cell Biology

Professional Activities:

1997 - present Member, NIH Study Section, Cell Biology and Physiology I
1998 - 2000 Editorial Board, Molecular and Cellular Biology
2000- present Associate Editor, Cancer Research

Publications (selected research articles from a total of 59)

Abate, C., Smith, J.A. and Joh, T.H. (1988). Characterization of the catalytic domain of bovine adrenal tyrosine hydroxylase. *Biochem. Biophys. Res. Comm.* 151:1446-1453.

Gentz, R., Rauscher III, F.J., **Abate**, C. and Curran, T. (1989). Parallel association of Fos and Jun leucine zippers juxtaposes DNA binding domains. *Science* 243:1695-1699.

Abate, C., Luk, D., Gentz, R., Rauscher III, F.J. and Curran, T. (1990). Expression and purification of the leucine zipper and DNA binding domains of Fos and Jun: Both Fos and Jun contact DNA directly. *Proc. Natl. Acad. Sci. USA* 87:1032-1036.

Abate, C., Luk, D. and Curran, T. (1990). A ubiquitous nuclear protein stimulates the DNA-binding activity of Fos and Jun indirectly. *Cell Growth & Differ.* 1:455-462.

Abate, C., Luk, D., Gagne, E., Roeder, R.G. and Curran, T. (1990). Fos and Jun cooperate in transcriptional regulation via heterologous activation domains. *Mol. Cell. Biol.* 10:5532-5535.

Abate, C., Patel, L., Rauscher III, F.J. and Curran, T. (1990). Redox regulation of Fos and Jun DNA-binding activity *in vitro*. *Science* 249:1157-1161.

Patel, L., **Abate**, C. and Curran, T. (1990). Altered protein conformation on DNA binding by Fos and Jun. *Nature* 347:572-575.

Abate, C. and Joh, T.H. (1991). Limited proteolysis of rat brain tyrosine hydroxylase defines an N-terminal region required for regulation of cofactor binding and directing substrate specificity. *J. Mol. Neurosci.* 2:203-215.

Abate, C., Luk, D. and Curran, T. (1991). Transcriptional regulation by Fos and Jun *in vitro:* Interaction among multiple activator and regulatory domains. *Mol. Cell. Biol.* 11:3624-3632.

Abate, C., Marshak, D.R. and Curran, T. (1991). Fos is phosphorylated by $p34^{cdc2}$, cAMP-dependent protein kinase and protein kinase C at multiple sites clustered within regulatory regions. *Oncogene* 6:2179-2185.

Baker, S.J., Kerppola, T.K., Luk, D., Vandenberg, M.T., Marshak, D.R., Curran, T. and **Abate**, C. (1992). Jun is phosphorylated by several protein kinases at the same sites modified in serum stimulated fibroblasts. *Mol. Cell Biol.* 12:4694-4705.

Catron, K.M., Iler, N. and **Abate**, C. (1993). Nucleotides flanking a conserved TAAT core dictate DNA binding specificity of three murine homeodomain proteins. *Mol. Cell. Biol.* 13:2354-2365.

Abate, C., Baker, S.J., Lees-Miller S., Anderson, C., Marshak, D.R. and Curran, T. (1993). Dimerization and DNA binding alter the phosphorylation of Fos and Jun. *Proc. Natl. Acad. Sci. USA* 90:6766-6770.

Shang, Z., Ebright, Y.W., Iler, N., Prendergast, P.S., Echelard, Y., McMahon, A.P., Ebright, R.H. and **Abate**, C. (1994). DNA affinity cleaving analysis of homeodomain-DNA interaction: Identification of homeodomain consensus sites in genomic DNA. *Proc. Natl. Acad. Sci. USA* 91:118-122.

Pellerin, I., Schnabel, C., Catron, K.M. and **Abate**, C. (1994). Hox proteins have different affinities for a consensus DNA site that correlate with the positions of their genes on the *hox* cluster. *Mol. Cell. Biol.* 14:4532-4545.

Shang, Z., Ebu Isaac, V., Li, H., Patel, L., Catron, K.M., Curran, T., Montelione, G. and **Abate**, C. (1994). Design of "minimAl" homeodomain: The N-terminal arm modulates DNA binding affinity and stabilizes homeodomain structure. *Proc. Natl. Acad. Sci. USA* 91:8373-8377.

Catron, K.M., Zhang, H., Marshall, S.C., Inostroza, J.A., Wilson, J.M. and **Abate**, C. (1995). Transcriptional repression by Msx-1 does not require homeodomain DNA binding sites. *Mol. Cell. Biol.* 15:861-871.

Ebu Isaac, V., Sciavolino, P. and **Abate**, C. (1995). Multiple amino acids determine the DNA binding specificity of the Msx1 homeodomain. *Biochemistry* 34:7127-7134.

Iler, N., Rowitch, D.H., Echelard, Y., McMahon, A.P. and **Abate-Shen**, C. (1995). A single homeodomain binding site restricts spatial expression of *Wnt-1* in the developing brain. *Mech. Dev.* 53:87-96.

Ebu Isaac, V., Patel, L., Curran, T. and **Abate-Shen**, C. (1995). Use of fluorescence resonance energy transfer to estimate intramolecular distances in the Msx-1 homeodomain. *Biochemistry* 34:15276-15281.

Zhang, H., Catron, K.M. and **Abate-Shen**, C. (1996). A role for the Msx-1 homeodomain in transcriptional regulation: Residues in the N-terminal arm mediate TATA binding protein interaction and transcriptional repression. *Proc. Natl. Acad. Sci. USA* 93:1764-1769.

Catron, K.M., Wang, H., Hu, G., Shen, M.M. and **Abate-Shen**, C. (1996). Comparison of Msx-1 and Msx-2 suggests a molecular basis for functional redundancy. *Mech. Dev.* 55:185-199.

Iler, N. and **Abate-Shen**, C. (1996) Rapid identification of homeodomain binding sites in the *Wnt-5a* gene using an immunoprecipitation strategy. *Biochem. Biophys. Res. Comm.* 227:257-265.

Schnabel, C.A. and **Abate-Shen**, C. (1996). Repression by HoxA7 is mediated by the homeodomain and the modulatory action of its N-terminal arm residues. *Mol. Cell. Biol.* 16:2678-2688.

Zhang, H., Hu., G., Wang, H., Sciavolino, P., Iler, N., Shen, M.M. and **Abate-Shen**, C. (1997). Heterodimerization of Msx and Dlx homeoproteins results in functional antagonism. *Mol. Cell Biol.* 17: 2920-2932.

Sciavolino, P.J., Abrams, E.W., Yang, L., Austenberg, L.P., Shen, M.M. and **Abate-Shen**, C. (1997). Tissue-specific expression of murine *Nkx3.1* in the male urogenital system. *Dev. Dynamics* 209:127-138.

He, W.W., Sciavolino, P., Wing, J., Augustus, M., Hudson, P., Meissner, P.S., Shell, B.K., Bostwick, D.G., Tindall, D.J., Gelmann, E.P., **Abate-Shen**, C. and Carter, K.C. (1997). A novel human prostate-specific, androgen-regulated homeobox gene (Nkx3.1) that maps to 8p21, a region frequently deleted in prostate cancer. *Genomics* 43:69-77.

Li, H., Tejero, R., Monleon, D., Bassolino-Klimas, D., **Abate-Shen**, C., Bruccoleri, R.E. and Montelione, G.T. (1997). Homology modeling using simulated annealing of restrained molecular dynamics and conformational search calculations with CONGEN: application in predicting the three-dimensional structure of murine homeobox domain Msx-1. *Protein Science* 6:956-970.

Bendall, A.J., Rincon-Limas, D.E., Botas, J., and **Abate-Shen**, C. (1998). Protein complex formation between Msx1 and Lhx2 homeoproteins is incompatible with DNA binding activity. *Differentiation.* 63:151-157.

Hu, G., Vastardis, H., Bendall, A.J., Wang, Z., Logan, M., Zhang, H., Nelson, C., Stein, S. Greenfield, N., Seidman, C.E., Seidman, J.G., and **Abate-Shen**, C. (1998). Haploinsufficiency of MSX1: A mechanism for selective tooth agenesis. *Mol. Cell Biol.* 18:6044-6051.

Yang, L., Zhang, H., Hu, G., Wang, H., **Abate-Shen**, C., and Shen, M. M. (1998). An early phase of embryonic Dlx5 expression defines the rostral boundary of the neural plate. *J. Neuroscience.* 18: 8322-8330.

Bhatia-Guar, R. Donjacour, A.A., Sciavolino, P.J., Kim, M., Desai, N., Young, P., Norton, C., Gridley, T., Cardiff, R.D., Cunha, G.R., **Abate-Shen**, C., and Shen, M.M. (1999). Roles for *Nkx3.1* in prostate development and cancer. *Genes Dev.* 13:966-977.

Bendall, A.J., Ding, J., Hu, G., Shen, M.M., and **Abate-Shen**, C. (1999). *Msx1* antagonizes the myogenic activity of *Pax3* in migrating limb muscle precursors. *Development* 126:4965-4976.

Yan, Y., Stein, S., Ding, J., Shen, M.M. and **Abate-Shen**, C. (2000). A novel PF/PN motif inhibits nuclear localization and DNA binding activity of the ESX1 homeoprotein. *Mol. Cell Biol.* 20:661-667.

Hu, G., Price, S., Shen, M.M. and **Abate-Shen**, C. *Msx1* inhibits cellular differentiation by upregulation of Cyclin D1.

Yan, Y.-T., Stein, S. M., Ding, J., Shen, M. M., and Abate-Shen, C. (2000). A novel PF/PN motif inhibits nuclear localization and DNA binding activity of the ESX1 homeoprotein. *Mol. Cell. Biol.*, 20:661-667.

Abate-Shen, C. and Shen, M.M. (2000) Molecular genetics of prostate cancer. *Genes Dev.* 14:2410-2434.

Bendall, A.J. and **Abate-Shen**, C. (2000) Roles for Msx and Dlx in vertebrate Development. Gene 247: 17-31.

Hu, G., Lee, H.,Price, S., Shen, M.M. and **Abate-Shen**, C. (2001) *Msx1* inhibits cellular differentiation by upregulation of Cyclin D1. *Development 128*: 2373-2384.

Selected recent reviews:

Sciavolino, P.J., and **Abate-Shen**, C. (1998). Molecular biology of prostate development and prostate cancer. *Annals of Medicine*. 30:357-368.

Bendall, A. J. and **Abate-Shen**, C. (2000). Roles for MSX and DLX homeoproteins in vertebrate development. *Gene.* 247:17-31.

Abate-Shen, C. and Shen, M. (2000). Molecular genetics of prostate cancer. *Genes Dev.* 14:2410-2434.

Cunha, G.R., Donjacour, A.A., Hayward, S.W., Thomsen, A., Marker, P., **Abate-Shen**, C., Shen, M.M., and Dahiya, R. (2000). Cellular and molecular biology of prostatic development. In *Prostate Cancer* (Kantoff, P. W., Carroll, P., D'Amico, Eds), A. Lippincott, Williams and Wilkins, Philadelphia, PA. In press.

(E-L) Immunohistochemical analysis of the anterior prostate of *Nkx3.1; Pten* compound mutants at 6 months of age. (E,F) Immunodetection of wide-spectrum cytokeratins (poly-cytokeratin; CK-P), which stains the cell surface of wild-type prostate epithelium (arrow). Note the high-level staining in the carcinoma *in situ* lesions of the *Nkx3.1*$^{+/-}$; *Pten*$^{+/-}$ prostate, suggestive of cytoskeletal reorganization. (G,H) Immunodetection of basal cells with CK14 (arrows), showing absence of basal cells in the interior of the carcinoma *in situ* lesions of the *Nkx3.1*$^{-/-}$; *Pten*$^{+/-}$ prostate. (I,J) Immunodetection of endothelial cells with CD105 (endoglin) showing increased microvascularization (J, arrows) of the carcinoma *in situ* lesions of the *Nkx3.1*$^{+/-}$; *Pten*$^{+/-}$ prostate. (K,L) Immunodetection with Ki67 antibody shows increased proliferative index in the carcinoma *in situ* lesions (arrows indicate positive cells). We note that the proliferative index of the unaffected epithelium in the *Nkx3.1; Pten* compound mutants was similar to that of the corresponding *Nkx3.1* single mutants, indicating that *Pten* heterozygosity does not significantly affect cellular proliferation. Scale bars represent 100 microns.

Figure 5: Absence of Nkx3.1 protein expression in mouse and human prostate cancer

(A-F) Immunochemical analysis of the anterior prostate of *Nkx3.1* and *Pten* mutants using a polyclonal antiserum that specifically detects the mouse Nkx3.1 protein. (A) Nkx3.1 immunostaining appears uniform in the epithelium of the *Nkx3.1*$^{+/+}$; *Pten*$^{+/+}$ prostate, while the adjacent stroma is unstained (arrow). *Inset* shows high-power view of nuclear staining of secretory cells, which is absent in the underlying basal cells (arrow). (B) Absence of Nkx3.1 immunostaining in a PIN region of a 12 month *Nkx3.1*$^{+/-}$; *Pten*$^{+/+}$ prostate, with uniform staining of the adjacent unaffected regions. *Inset* shows high-power view of unstained and stained nuclei at the margin of the PIN region (arrow). (C,D) Absence of Nkx3.1 immunostaining in a small carcinoma *in situ* lesion of a 6 month *Nkx3.1*$^{+/+}$; *Pten*$^{+/-}$ prostate (C, arrow) and a large carcinoma *in situ* lesion of an 8 month *Nkx3.1*$^{+/-}$; *Pten*$^{+/-}$ prostate (D, arrow). Note that the adjacent unaffected regions in (C) display uniform immunostaining. *Inset* in D shows unstained nuclei with atypia and mitotic figure (arrow). (E) Heterogeneity of Nkx3.1 immunostaining (arrows) in a histologically unaffected region of an 8 month *Nkx3.1*$^{+/-}$; *Pten*$^{+/-}$ prostate. *Inset* shows high-power view of the juxtaposition of stained, unstained, and lightly-stained nuclei. (F) Example of cytoplasmic Nkx3.1 immunostaining at the margins of a large carcinoma *in situ* lesion of an 12 month *Nkx3.1*$^{+/-}$; *Pten*$^{+/-}$ prostate. *Inset* shows high-power view of the cytoplasmic staining (arrow).

(G-I) Immunohistochemical analysis of human prostatectomy specimens using a polyclonal antiserum that specifically detects the human NKX3.1 protein. (G) Example of NKX3.1 immunostaining of normal prostate epithelium (NPE). Note absence of staining in the basal cells (arrows) and adjacent stroma. *Inset* shows high-power view of nuclear staining of secretory epithelial cells (arrow). (H) Absence or heterogeneous NKX3.1 immunostaining in a well-differentiated cancer (CaP), compared with adjacent NPE. *Inset* High power view showing absence of staining in the cancer cells (arrow). Note that the absence of a basal layer in the cancer ducts. (I) Predominantly cytoplasmic NKX3.1 immunostaining of a poorly differentiated cancer (arrows). *Inset* High power view of cytoplasmic staining (Arrows).

(J-L) Immunochemical analysis of the anterior prostate of *Pten* and *Nkx3.1; Pten* mutants using a polyclonal antiserum that detects the mouse Pten protein. (J) Uniform immunostaining in the epithelium and stroma of the *Nkx3.1*$^{+/+}$; *Pten*$^{+/+}$ prostate. (K) Moderate reduction of Pten immunostaining in a small carcinoma *in situ* lesion of a 5 month *Nkx3.1*$^{+/+}$; *Pten*$^{+/-}$ prostate (arrows). (L) Absence of Pten immunostaining in a relatively large carcinoma *in situ* lesion of a 12 month *Nkx3.1*$^{+/-}$; *Pten*$^{+/-}$ prostate. In K and L, note that immunostaining of the adjacent histologically unaffected regions is similar to wild-type (J). Scale bars in A-L represent 100 microns.

(M-O) Analysis of the allelic status of *Nkx3.1* and *Pten* in carcinoma *in situ* lesions of the *Nkx3.1*$^{+/-}$; *Pten*$^{+/-}$ anterior prostates. (M) Laser-capture microdissection was performed on Nkx3.1-immunostained sections to isolate genomic DNA from carcinoma *in situ* lesions (Nkx3.1-non-expressing) and adjacent unaffected regions (Nkx3.1-expressing). The genomic DNA was analyzed by PCR followed by Southern blotting. 20 independent lesions and 8 unaffected regions were analyzed; representative data from 6 lesions (1-6) and 1 control are shown. (N,O) Southern blot analysis to detect the wild-type (WT) alleles for *Nkx3.1* and *Pten*; detection of the targeted allele (KO) serves as an internal control.

Figure 6: Loss-of-function of *Nkx3.1* and *Pten* converge on Akt activation

(A) Western blot analysis shows high levels of activated Akt in protein extracts from the anterior prostate (lanes 1-4), but not the bladder (lanes 5-8), of *Nkx3.1; Pten* compound mutants at 8 months of age. Protein lysates (20 μgs) were resolved on 10% PAGE gels and probed with antisera to detect activated Akt (phospho-Akt; α-pAkt), total Akt (α-Akt), Pten or Nkx3.1. Note the reduced levels of Pten in the *Nkx3.1*$^{-/-}$; *Pten*$^{+/-}$ compound mutants relative to the *Pten*$^{+/-}$ single mutants.

(B) (Top) Western blot analysis of whole cell (W), cytoplasmic (C) and nuclear (N) extracts from LNCaP human prostate carcinoma cells infected with *Nkx3.1*-expressing or control (vector) retroviruses. Note that total Akt protein (α-Akt) is enriched in the cytoplasmic fraction, while Nkx3.1 protein (α-Nkx3.1) is in the nuclear fraction. (Bottom) Akt kinase activity was examined following immunoprecipitation with α-Akt, using GSK-3 as a substrate. Western blot analysis was performed using α-phospho-GSK3α/β.

(C-H) Immunohistochemical analysis of the distribution of phospho-Akt immunostaining in the anterior prostates of *Nkx3.1* and *Pten* mutants. (C) Low-power view shows absence of staining in the wild-type prostate. (D) Robust staining in small patches of cells of the *Nkx3.1*$^{+/+}$; *Pten*$^{+/-}$ prostate at 5 months (arrows) *Inset* shows high-power view of the area marked by the arrow. (E) Robust staining in the carcinoma *in situ* lesions of the *Nkx3.1*$^{-/-}$; *Pten*$^{+/-}$ prostate at 5 months. *Inset* shows high-power view. (F-G) Low-power and high-power views show examples of phospho-Akt immunostaining (arrows) in clusters of cells in the *Nkx3.1*$^{-/-}$ prostates at 15 (F) or 7 (G,H) months. Panel F (and *inset*) show examples of staining at the cell surface; Panel H (and *inset*) show examples of nuclear staining.

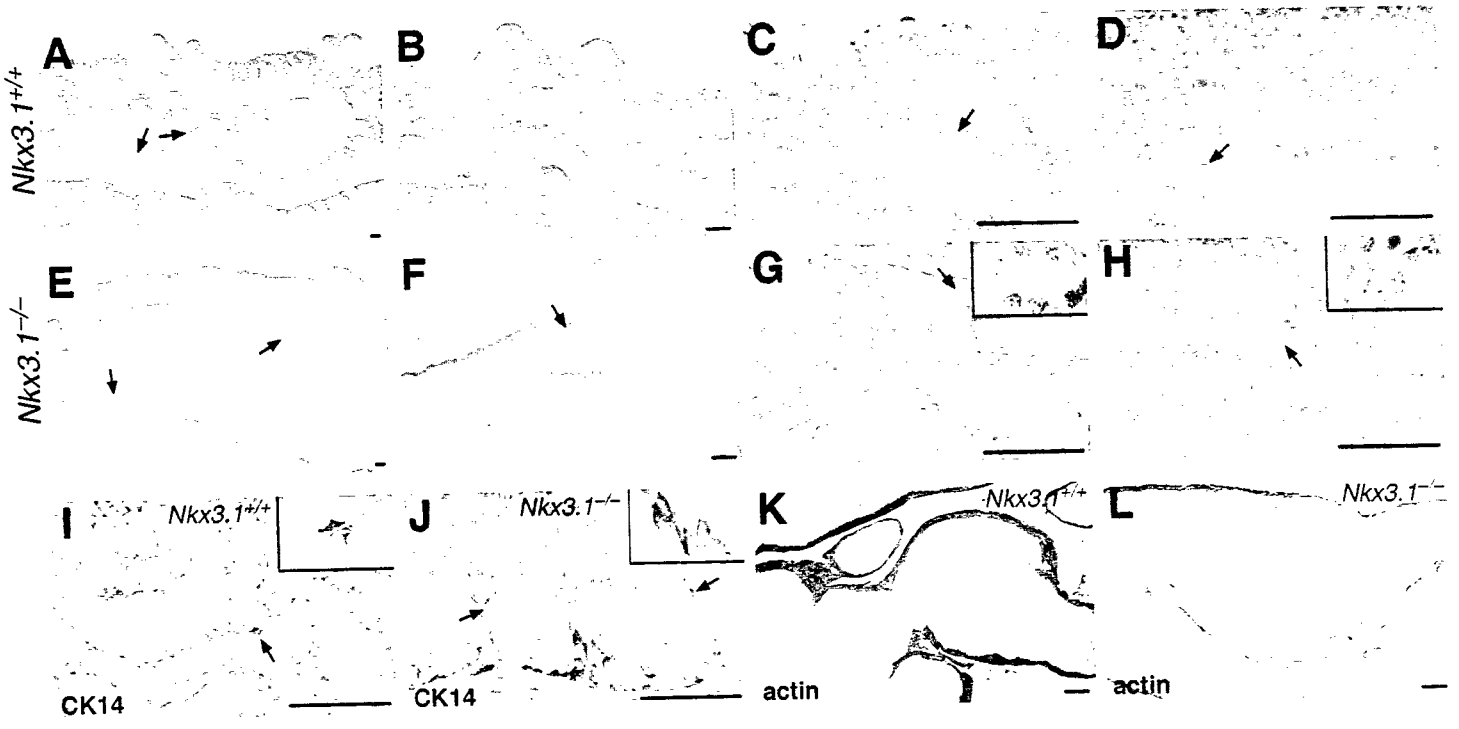
A
B
C
D
Nkx3.1+/+
E
F
G
H
Nkx3.1−/−
I
Nkx3.1+/+
J
Nkx3.1−/−
K
Nkx3.1+/+
L
Nkx3.1−/−
CK14
CK14
actin
actin

Figure 1

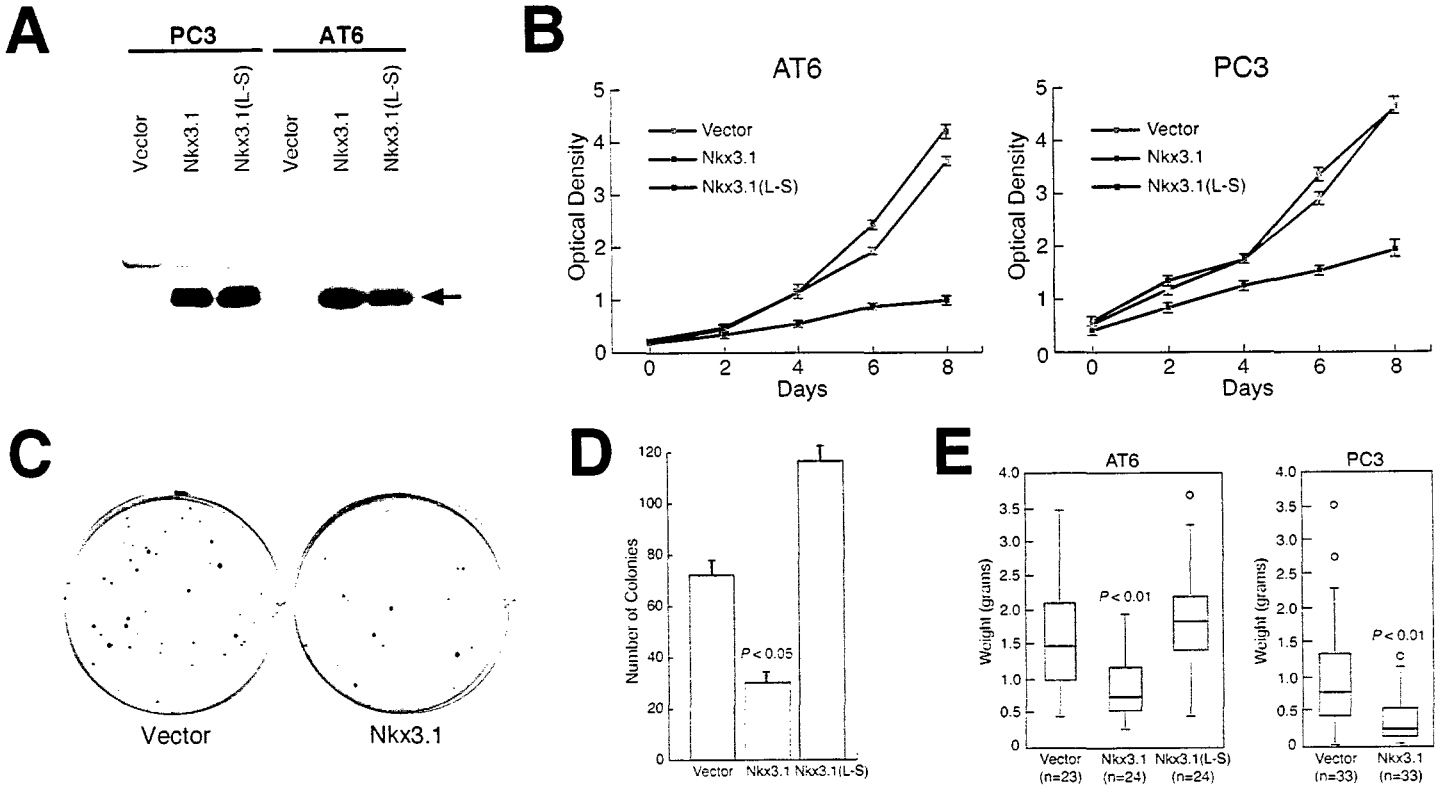
A
PC3
AT6
Vector
Nkx3.1
Nkx3.1(L-S)
Vector
Nkx3.1
Nkx3.1(L-S)
B
AT6
PC3
Optical Density
Days
Vector
Nkx3.1
Nkx3.1(L-S)
C
Vector
Nkx3.1
D
Number of Colonies
P < 0.05
Vector
Nkx3.1
Nkx3.1(L-S)
E
AT6
PC3
Weight (grams)
P < 0.01
P < 0.01
Vector (n=23)
Nkx3.1 (n=24)
Nkx3.1(L-S) (n=24)
Vector (n=33)
Nkx3.1 (n=33)

Figure 2

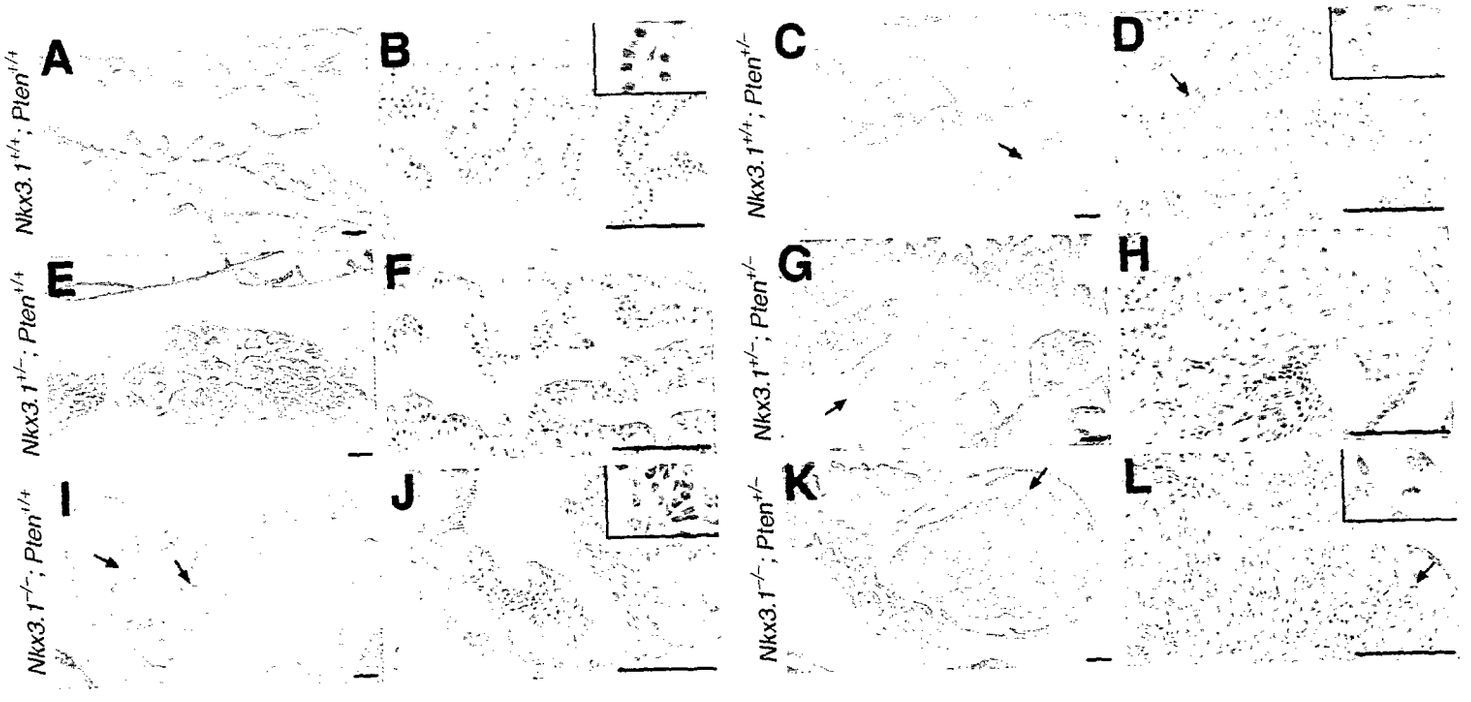
A
B
C
D
E
F
G
H
I
J
K
L
Nkx3.1+/+; Pten+/+
Nkx3.1+/+; Pten+/−
Nkx3.1+/−; Pten+/+
Nkx3.1+/−; Pten+/−
Nkx3.1−/−; Pten+/+
Nkx3.1−/−; Pten+/−

Figure 3

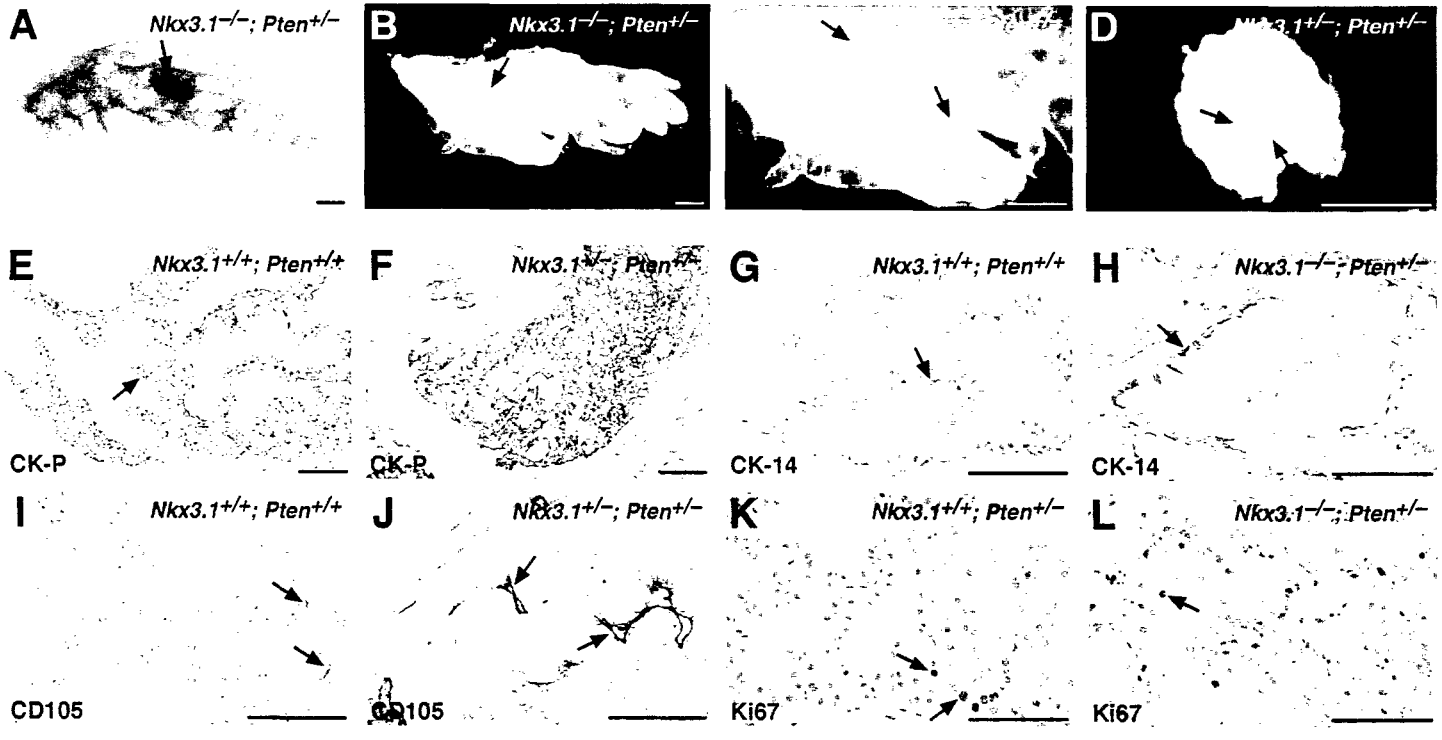
A
Nkx3.1−/−; Pten+/−
B
Nkx3.1−/−; Pten+/−
D
E
Nkx3.1+/+; Pten+/+
CK-P
F
Nkx3.1+/−; Pten+/−
CK-P
G
Nkx3.1+/+; Pten+/+
CK-14
H
Nkx3.1−/−; Pten+/−
CK-14
I
Nkx3.1+/+; Pten+/+
CD105
J
Nkx3.1+/−; Pten+/−
CD105
K
Nkx3.1+/+; Pten+/−
Ki67
L
Nkx3.1−/−; Pten+/−
Ki67

Figure 4

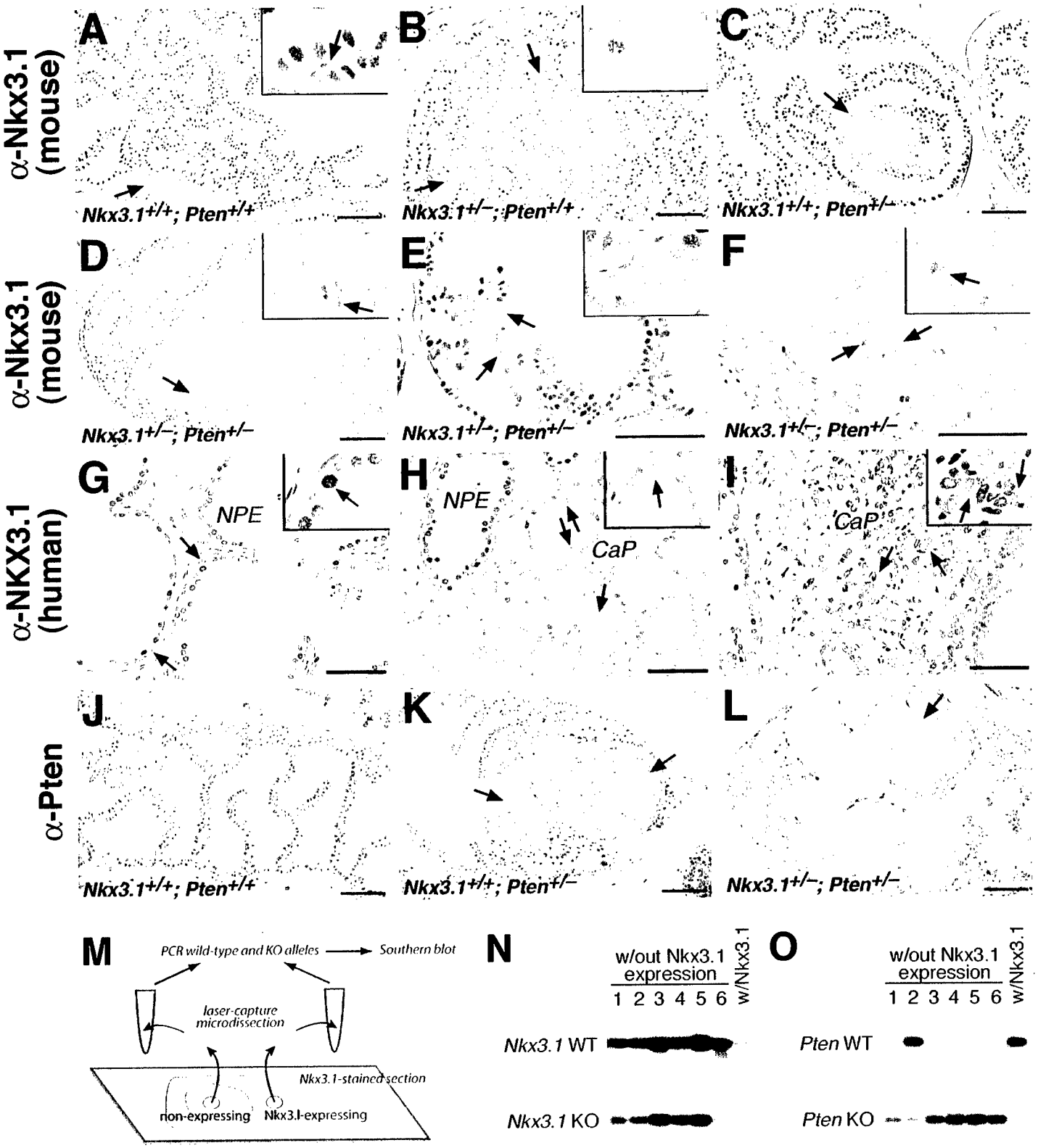
α-Nkx3.1 (mouse)
α-Nkx3.1 (mouse)
α-NKX3.1 (human)
α-Pten
A
B
C
D
E
F
G
H
I
J
K
L
Nkx3.1+/+; Pten+/+
Nkx3.1+/−; Pten+/+
Nkx3.1+/+; Pten+/−
Nkx3.1+/−; Pten+/−
Nkx3.1+/−; Pten+/−
Nkx3.1+/+; Pten+/+
Nkx3.1+/+; Pten+/−
Nkx3.1+/−; Pten+/−
NPE
NPE
CaP
CaP
M
PCR wild-type and KO alleles
Southern blot
laser-capture microdissection
Nkx3.1-stained section
non-expressing
Nkx3.1-expressing
N
w/out Nkx3.1 expression
1 2 3 4 5 6
w/Nkx3.1
Nkx3.1 WT
Nkx3.1 KO
O
w/out Nkx3.1 expression
1 2 3 4 5 6
w/Nkx3.1
Pten WT
Pten KO

Figure 5

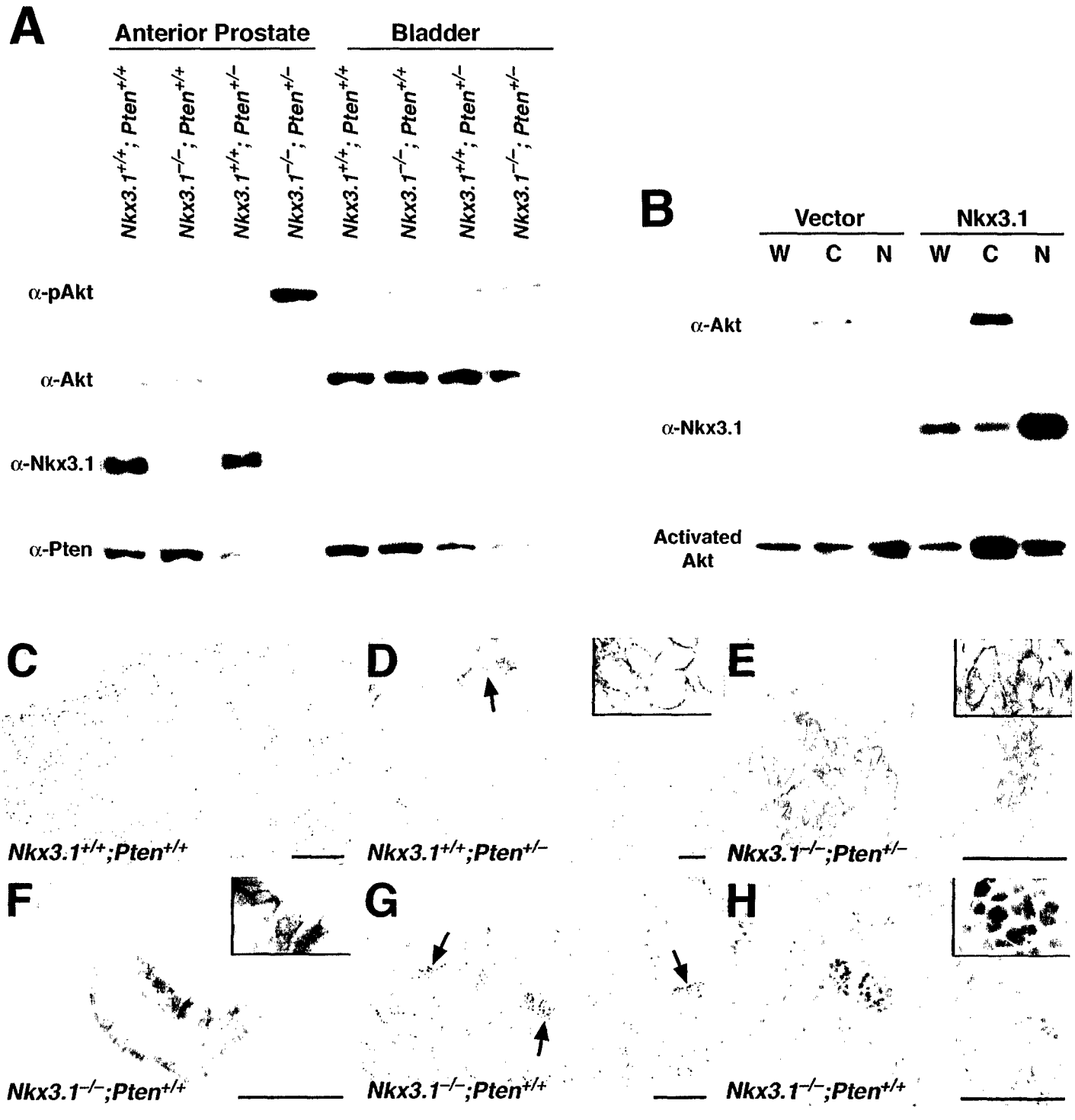
A
Anterior Prostate
Bladder
Nkx3.1+/+; Pten+/+
Nkx3.1−/−; Pten+/+
Nkx3.1+/+; Pten+/−
Nkx3.1−/−; Pten+/−
Nkx3.1+/+; Pten+/+
Nkx3.1−/−; Pten+/+
Nkx3.1+/+; Pten+/−
Nkx3.1−/−; Pten+/−
α-pAkt
α-Akt
α-Nkx3.1
α-Pten
B
Vector
Nkx3.1
W C N W C N
α-Akt
α-Nkx3.1
Activated Akt
C
D
E
Nkx3.1+/+;Pten+/+
Nkx3.1+/+;Pten+/−
Nkx3.1−/−;Pten+/−
F
G
H
Nkx3.1−/−;Pten+/+
Nkx3.1−/−;Pten+/+
Nkx3.1−/−;Pten+/+

Figure 6